IJE TRANSACTIONS B: Applications Vol. 32, No. 11, (November 2019) 1665-1680

International Journal of Engineering

Journal Homepage: www.ije.ir

Energy and Exergy Evaluation of Multi-channel Photovoltaic/Thermal Hybrid System: Simulation and Experiment

A. Hosseini Rad[a], H. Ghadamian*[a], H. R. Haghgou[a], F. Sarhaddi[b]

[a] *Department of Energy, Materials and Energy Research Center (MERC), Tehran, Iran*
[b] *Department of Mechanical Engineering, University of Sistan and Baluchestan, Zahedan, Iran*

PAPER INFO

Paper history:
Received 22 July 2019
Received in revised form 17 August 2019
Accepted 12 September 2019

Keywords:
Computational Modeling
Exergy and Energy Analysis
Multichannel System
Laminar and Turbulent Flows
Photovoltaic/ Thermal

ABSTRACT

In this research, a pilot study and analysis of an innovative multi-channel photovoltaic/thermal (MCPV/T) system in a geographic location (35° 44' 35" N, 50° 57' 25" E) has been carried out. This system consists of integrating a photovoltaic panel and two PV/T heat-sink converters. The total electrical, exergy and energy efficiencies of the system at air flow rate of 0.005 kg/s and radiation intensity of 926 w/m^2 were 9.73%, 10.72%, and 47.24%, respectively. An air flow rate of 0.011 kg/s and the radiation intensity of 927 w/m^2 were also achieved to be 9.35%, 10.40% and 65.10%, respectively. Based on simulation results considering experiments validations, as the air flow rate increases, the overall energy efficiency increases to the maximal amount of 80%. However, the maximum exergy efficiency value has a local optimal point of 13.46% at a fluid flow rate of 0.024 kg/s. Similarly, with increasing channel heights, the total energy efficiency decreased to 70%, and the maximum exergy efficiency has a local optimal point of 13.64% at channel height of 0.011 m. As an overall achievement, the system has higher energy quality (exergy efficiency) in laminar flow regime and has higher energy efficiency under turbulent flow conditions.

***doi**: 10.5829/ije.2019.32.11a.18*

NOMENCLATURE

a	Ideality factor (eV)	ρ	Density (kg/m^3)
A_{mod}	PV module area (m^2)	**Greek Symbols**	
b	The width of MCPV/T (m)	α	Absorptivity, Current temperature Coefficient (mA/°C)
C_f	The conversion factor of a thermal power plant (-)	β	Packing factor, Voltage temperature coefficient (V/°C)
C_P	Specific heat capacity of air (J/kg.K)	$(\alpha\tau)_{eff}$	The product of effective absorptivity and transmissivity (-)
dx	Elemental Length of flow duct (m)	ε	Emissivity (-)
dy	Elemental Length of fin (m)	η	Efficiency (%)
$\dot{E}_Q$	Exergy rate (W)	σ	Stefan-Boltzmann's constant (W/m^2.K^4)
$\dot{E}_{X_Q}$	Heat transfer Exergy rate (W)	τ	Transmittivity (-)
$\dot{E}_{X_w}$	Work Exergy rate (W)	Δ	Difference in temperature, pressure (-)
Error	Error rate of reply convergence (-)	**Subscripts**	
F'	Collector efficiency coefficient (-)	*A*	Air
F_R	Heat removal factor (-)	*Al*	Aluminum
G	Solar radiation intensity (W/m^2)	*Amb*	ambient
h	Convective heat transfer coefficient (W/m^2.K)	*Bs*	Back surface of tedlar
h_p	Penalty factor (-)	*Cell*, *c*	Solar Cell

*Corresponding Author Email: *h.ghadamian@merc.ac.ir* (H. Ghadamian)

Please cite this article as: A. Hosseini Rad, H. Ghadamian, H. R. Haghgou, F. Sarhaddi, Energy and Exergy Evaluation of Multi-channel Photovoltaic/Thermal Hybrid System; Simulation and Experiment, International Journal of Engineering (IJE), IJE TRANSACTIONS B: Applications Vol. 32, No. 11, (November 2019) 1665-1680

H	Duct depth (m)	*Cond*	Conductive
$\dot{I}_{cv}$	Irreversibility Rate (W)	*Conv*	Convective
I	Circuit Current (A)	*D*	Diode
k	conductive heat transfer coefficient (W/m.K)	*El*	Electrical
l	Length of flow duct (m), Thickness (m)	*Ex*	Exergy
L_C	Corrected length of fin (m)	*Exp*	Experimental
L_1	Length of PV module (m)	*F*	Working Fluid
L_2	Width of PV module (m)	*Fan*	Duct Fan
m	Aluminum fin parameter (m^{-1})	*G*	Glass
$\dot{m}$	Fluid flow rate (kg/s)	*In*	Inlet
n	Number of experiment (-)	*L*	Light Current
N_C	Number of channels per heat exchanger (-)	*Mp*	Maximum power point
N_H	Number of heat exchangers (-)	*O*	Reverse saturation
Nu_D	Nusselt number (-)	*OC*	Open-circuit
p	Pressure (N/m^2), Power (w)	*Out*	Outlet
pr	Prandtl number (-)	*Ov*	Overall
$\dot{Q}$	Heat transfer rate (w)	*Rad*	Radiative
R	Resistance (Ω), Gas constant (kj/kg.K)	*Ref*	Reference
Re_D	Reynolds number (-)	*S*	series
t_d	Thickness of duct (m)	*Sc*	Short-circuit
T	Temperature (K)	*Sh*	Shunt
U_t	Total heat loss coefficient from Cell to Ambient ($W/m^2.K$)	*Si*	Silicon
U_T	Total heat transfer coefficient from cell to tedlar ($W/m^2.K$)	*Sim*	Simulated
V	Circuit Voltage (V), Wind Velocity (m/s)	*T*	Tedlar
W	Width of flow duct (m)	*Th*	Thermal
X	Experimental or simulated value of parameter (-)	*U*	useful

1. INTRODUCTION

It is well-known that photovoltaic (PV) module efficiency decreases by 0.45% for every degree increase in solar cells temperature [1, 2]. This fact is due to a huge amount of solar radiation on PV module that are not converted to electricity, while the PV module temperatures can raise to 80 °C especially in the summer [3]. Regarding this issue, hybrid PV/thermal collectors (PV/T) is introduced which is capable of generating thermal and electrical energy simultaneously [4]. In other words, a heat carrier fluid removes the additional excess heat of photovoltaic cells. Consequently, cells face-up operate at downgrade temperature and lead the system to achieve higher performance regards to more generating in electrical power [5, 6].

Kern and Russell were the first to present the basic concept of photovoltaic heat collectors operated by two-fluid mediums with laboratory results [7]. Tripanagnostopoulos [8] states that when the fluid medium of air is used in the PV/T system, the type of contact of the air with the back surface of Tedlar PVF Film is direct and in the case where water fluid is used, the contact is indirect due to the lower heat capacity of air compared to water. De Soto et al. [9] have worked to model and simulate the current-voltage behavior of the solar cell in real experimental situations. Zondag et al. [10] numerically modeled the PV/T system with the fluid medium of the water using the finite difference method and concluded that a simple one-dimensional static model has a desirable accuracy to check the performance of the system during a day. Tiwari et al. [11] contributed to the analytical solution of the PV/T collector with the fluid medium of air which had an appropriate agreement with the laboratory test results. Joshi et al. in a similar study to Joshi et al. [12] investigated two types of photovoltaic modules, including photovoltaic modules for Glass-Glass and Glass-Tedlar. The electrical efficiency of the two systems was equal, but the higher total efficiency of the first system was reported. Sarhaddi et al. [13] provided an analytical solution in a steady and one-dimensional state of single-channel PV/T system with air-fluid medium. They used an improved electric model to analyze the electrical part of the system. In addition, using the appropriate heat transfer coefficients, the thermal modeling of the system was in good agreement with the laboratory values of other papers.

Amori and Taqi Al-Najjar [14] in a similar activity with Sarhaddi et al., developing a better thermal and electrical modeling, they tested a laboratory PV/T system with an air-fluid medium in the summer and winter seasons and they reported better system performance in the winter than summer. Tonui and Tripanagnostopoulos [15] experimentally investigated three different PV/T systems with air-fluid medium including a single-channel PV/T system, PV/T system with a thin metal plate as an adsorbent and a PV/T system with a finned absorber The thermal efficiency of the three systems was 25, 28 and 30%, respectively.

In order to increase the thermal and electrical efficiency of the PV/T system, the researchers have investigated the exergy efficiency of the PV/T system using analytical and numerical solution methods. In fact, exergy is a way to find the quality of energy produced by the system. Petela [16] has given a new expression of the amount of exergy received from solar energy He compared the relationship reported in his study with previous relationships and presented Bijan's view [17] on the various views of the solar exergy. Chow et al. provided numerical modeling and laboratory testing of two PV/T system samples with a water fluid medium coated with glass and without glass coating. Based on their results, if the design goal is total or quantitative energy, the case with glass coating has higher efficiency, and if the design objective is exergy or quality, then the glass-free mode has higher efficiency.

Sarhaddi et al. [18] modeled the exergy efficiency of the PV/T collector with air-fluid medium. They used the concept of exergy degradation as well as the pure exergy input to find exergy efficiency. Sobhnamayan et al. [19] examined the energy and exergy of the PV/T system with air-fluid medium. They used a new model to calculate the exergy efficiency and compared the simulation results with the experimental results that were in appropriate confirmations. Joshi and Tiwari investigated the efficiency of PV/T collectors in terms of energy and exergy which showed the energy efficiency of about 55~56% and exergy efficiency of about 12~15% [20].

In recent years, the studies are focused on the different geometries of channels to investigate their effects on the efficiency of PV/T systems. Robles et al. [21] investigated a solar water heater system, a heat converter which consists of parallel rectangular channels with a small hydraulic diameter and had a 13% more efficiency compared to the flat panel solar collector [21]. Jin et al. [22] experimentally investigated two PV/T systems including a heat converter with parallel rectangular channels and with a flat panel air collector using air-fluid medium They reported in different flow rates, the optimal flow rate was 0.0287 kg/s to achieve maximum efficiency. Tabet et al. [23] used a heat converter similar to reported data [21, 22], out of 5, 10, and 15 flow channels to analyzed a PV/T system with air-fluid medium. In this study, 15 channels were described as optimal for receiving the maximal amount of energy efficiency. Fan et al. [24] investigated the dynamics and solving of governing equations using the Crank–Nicolson method for a PV/T system similar to reported data [22, 23], which are connected to a solar-powered air heater in series mode. They finally compared the response of modeling the system stable state and dynamical mode-modeling and reported that a stable state response could well predict the behavior of the system. Srinivas and Jayaraj [25] studied experimentally a new design of double pass hybrid (PV/T) solar air heater with slats (DPHSAH). The average values for electrical, thermal and overall efficiencies achieved 3.9, 18 and 28%, respectively while the mass flow rate had been considered equal to 0.0123 kg/s. In the research done by Teo et al. [26] both experimental and numerical analysis was applied to study the effects of active and passive cooling by air. Based on their research outcomes, the uniformity of the temperature distribution increase in order to the new designed manifold. Furthermore, by analyzing the effects of mass flow rate on both electrical and thermal efficiency, it was concluded that the maximum possible value for both efficiencies can be obtained in the flow rate of 0.08 kg/s.

By the reviewed references, it is found that the PV/T system can be considered as the best response to consumer thermal and electrical energy compared to individual systems. In the case of the PV/T system with air-fluid medium, one of the challenges is to increase the overall system efficiency by taking into account the quantity of energy. Further researchers have long been investigating the factors affecting the thermal and electrical behavior of the PV/T system without precise considering the increase in overall efficiency. Just in few cases, the response of these variables has been analyzed on overall energy efficiency and exergy.

To overcome the mentioned shortages, in this research the development of static modeling and a novel accurate solution of a MCPV/T system with multi-flow channels as well as validation of the equations obtained with experimental results have been considered which is completely different from the numerical method stated in literature [22–24]. The contact of air to the back surface of Tedlar PVF Film is direct and a novel fan positioning is considered in the middle of the system. A comprehensive study regarding parametric analysis has been conducted and the effect of fan positioning, fluid flow rate and flow channel height on energy and exergy efficiency of the system have been also investigated. In other words, in addition to studying the effect of variables affecting the behavior of the PV/T system with the air-fluid-medium, in this study an innovative thermal converter sample was used to increase the overall efficiency of the system with the energy quantity view. A novel accurate solution of a MCPV/T system has been used to investigate the thermal response of the system which leads to the production of an equation that

researchers can easily use to predict the behavior of the system. In a short viewpoint, this research project is implemented in the following steps:

- Coding and simulation to find a differential solution,
- A novel multi-channel heat-sink design & produce as sub-systems and assembling,
- Monitoring, measurement and final validation,
- Parametric analysis to achieve system variation behavior.

2. SYSTEM DESIGN AND MEASUREMENT CONDITIONS

In this step, steady-state differential scale simulation is done to achieve the analytical solution. A novel accurate solution and finding system profiles are a major strength of this study simulation section. A different element of the PV/T is demonstrated in Figure 1. The components of the multichannel thermal photovoltaic system made in this study include photovoltaic panels, heat-sink convertor, fans, input and output entries for fluid flow. Under the photovoltaic panel, there are two multichannel heat-sink convertors in direct contact with the back surface of Tedlar PVF Film. There is a gap of 4 centimeters between the two heat-sink converters and in the longitudinal center of the system. The entry of the airflow is for installing the suction fans. Three fans with 4×4 cm dimensions and technical specifications of 0.16 amps and 12 volts have been installed in this location, as shown in the schematic diagram. Each PV/T heat-sink converter includes 16 airflow aluminum channels. The heat transfer mechanism of the airflow and the aluminum channel with Tedlar back surface are convection and conduction, respectively. In fact, due to the low thermal air capacity of the air, it is in direct contact with the Tedlar back surface to increase the amount of heat transfer fluid in the air.

Within the second step, a novel heat sink is designed and produced as sub-systems and further assembling of system parts are demonstrated in Figure 2. Figure 2, a workshop-sample-product of aluminum flow channels, an assemblage of aluminum channels beneath the photovoltaic panel, fans installation in the fluid flow outlet or middle positions and a completed system sample under sunlight test conditions are observed. As you can be seen in Figure 2, heat converters have been assembled directly beneath the Tedlar. Then, a PVC insulation layer was used for heat insulation behind the aluminum channels. The designed system has been installed in a geographic location with coordinates (35° 44' 35" N, 50° 57' 25" E) and has an angle of 35 degrees from the horizon and facing the south. The performance of the system has been measured and analyzed for two different modes of flow rate during the consecutive days of July to October 2017 under clear sunlight sky conditions. In

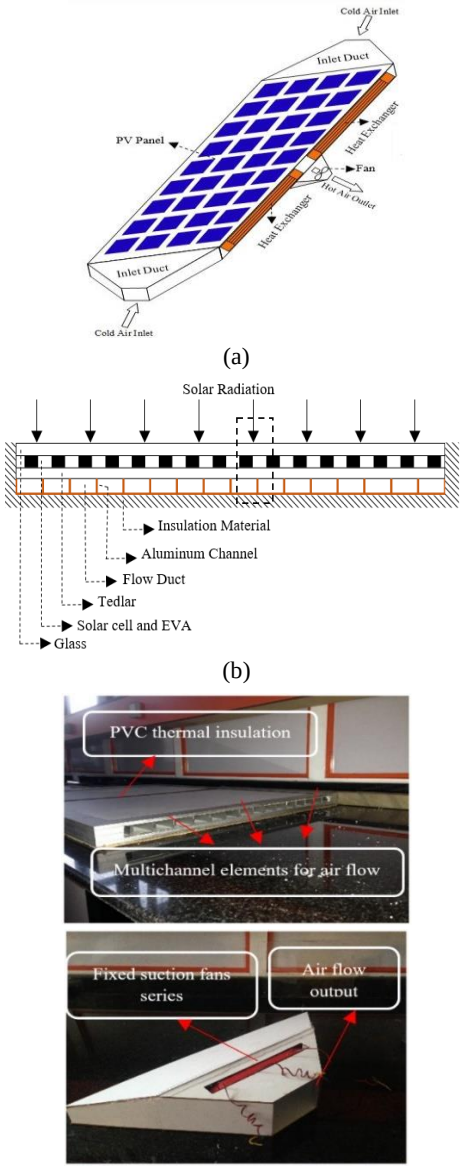

Figure 1. A schematic of a designed MCPV/T system. (a): Side view, (b): Cross-section view and (c): Sub-systems

order to monitor the system's operation in a uniform flow mode, the Urban Electricity Grid has been used to set up and control system fans instead of directly using the photovoltaic panel output power. In the equations of electrical efficiency, the fans power system consumptions are also included. The used instruments in the experimental measurement are introduced in Table 1.

3. COMPUTATIONAL MODELING

3. 1. Thermal Modeling Schematic Figure 3-a magnifies the dashed line part in Figure 2. This figure represents the different layers of the system for a flow

channel. The temperature of the various layers is shown beside an equivalent thermal resistance configuration plotted for the flow channel in Figure 3-b.

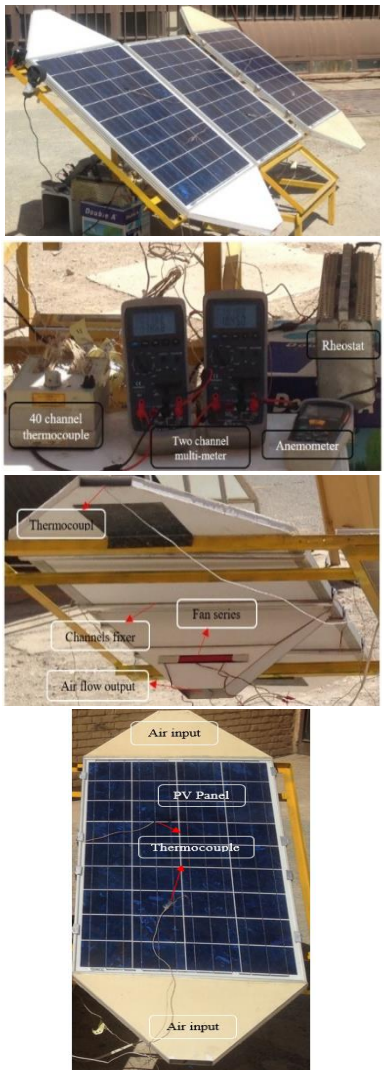

Figure 2. Assembled MCPV/T system at environmental test conditions

TABLE 1. Used instruments in the experimental measurement and their resolution

Instrument	Accuracy of measurement
ST-8891E contact thermometer	0.1 ℃
DT-8863B Infra Red Thermometer	0.1 ℃
Hot-Wire Anemometer TES-1341	0.1 ℃
CFM/CMM Thermo Anemometer Model DT-619	0.1 m/s
Digital Multi-Meter PROVA 803	0.1% DC voltage basic accuracy and 0.2% AC voltage basic accuracy
Solar Power Meter TES-1333R	0.1 W/m^2

Based on Figure 3, an analytic solution develops. The results are shown in Table 2. Based on the extracted equation in Table 2 an open-source-code simulation of the system is developed in MATLAB software. By developing the energy balance equations for the multi-channel PV/T system, the temperature of the different points, the thermal efficiency of the system and the dependent and independent coefficients will be according to Tables 2 and 3. For more details, extensive discussion reported in literature [11–14, 27, 28].

3. 2. Electrical Analysis It is necessary to explain the electric analysis model for the simulation process. In this study, a five-parameter model is applied to introduce the I-V characteristic curve of a solar cell which is presented in Table 4. The equivalent electrical circuit of the five-parameter model is demonstrated in Figure 4.

To solve the nonlinear equation of solar cell behavior (Equation (20), the following five constraints according to Equations (21) to (25) shown in Table 4 are required to be considered. By replacing the constraints in Equation (20), all governing equations will be transformed into the nonlinear system of five independent variables equations using the Newton-Raphson algorithm to solve nonlinear equations system. In new functional conditions (G_{new},$T_{cell,new}$), according to literature [8, 11, 15] a series of transport equations are applied. The electrical efficiency of the MCPV/T system is defined as the maximum useful electric power produced (output) by the photovoltaic panel divided by the irradiation energy received by the surface of the collector cells according to Equation (26).

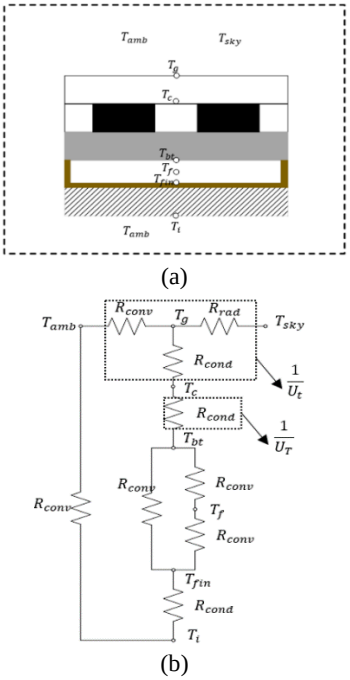

Figure 3. (a): The different layers of a flow channel and (b): The equivalent thermal resistance circuit

TABLE 2. The system temperatures governing equations, the useful heat energy rate and the system thermal efficiency [11–14]

Title	Equation	No.
Solar Cell Temperature	$T_{cell}=\frac{U_T T_{bs}+U_t T_{amb}+(\alpha\tau)_{eff}G}{U_T+U_t}$	(1)
Back Surface Temperature of Tedlar	$T_{bs}=T_f+\frac{[U_{tT}(T_{amb}-T_f)+h_p(\alpha\tau)_{eff}G]w}{h_{f,T-a}(w-2t_d)+2k_{Al}mt_d\tanh(mL_c)+U_{tT}w}$	(2)
Outlet Air Temperature	$T_{f,out}=\left[T_{amb}+\frac{h_p(\alpha\tau)_{eff}G}{U_{tT}}\right]\left[1-exp\left(\frac{-bF'U_{tT}}{\dot{m}c_p}L\right)\right]+T_{f,in}exp\left(\frac{-bF'U_{tT}}{\dot{m}c_p}L\right)$	(3)
Average Temperature of air	$\bar{T}_f=\frac{1}{L}\int_{x=0}^{L}T_f(x)dx=\left[T_{amb}+\frac{h_p(\alpha\tau)_{eff}G}{U_{tT}}\right]\left[1-\frac{1-exp\left(\frac{-bF'U_{tT}}{\dot{m}c_p}L\right)}{\frac{bF'U_{tT}}{\dot{m}c_p}L}\right]+\frac{1-exp\left(\frac{-bF'U_{tT}}{\dot{m}c_p}L\right)}{\frac{bF'U_{tT}}{\dot{m}c_p}L}T_{f,in}$	(4)
Useful Heat Energy Rate	$\dot{Q}_u=\dot{m}C_p(T_{f,out}-T_{f,in})=F_R bL[h_p(\alpha\tau)_{eff}G-U_{tT}(T_{f,in}-T_{amb})]$	(5)
Thermal Efficiency	$\eta_{th}=\frac{\dot{Q}_u}{bLG}=F_R\left[h_p(\alpha\tau)_{eff}-\frac{U_{tT}(T_{f,in}-T_{amb})}{G}\right]$	(6)

TABLE 3. The dependent coefficients to couple with Table 2 variables [27, 28]

Title	Equation	No.
The product of effective absorptivity and transmissivity	$(\alpha\tau)_{eff}=\tau_g[\alpha_c\beta_c+\alpha_T(1-\beta_c)-\beta_c\eta_{ele}]$	(7)
Penalty factor	$h_p=\frac{U_T}{U_T+U_t}$	(8)
An overall heat transfer coefficient from glass to Tedlar through the solar cell	$U_{tT}=\frac{U_T U_t}{U_T+U_t}$	(9)
Aluminum fin factor	$m=\sqrt{\frac{h_{f,Al-a}}{t_d k_{Al}}}$	(10)
An overall heat transfer coefficient from the solar cell to ambient through the glass cover	$U_t=\left[\frac{L_g}{k_g}+\frac{1}{h_{conv}+h_{rad}}\right]^{-1}$	(11)
A conductive heat transfer coefficient from the solar cell to flowing air through Tedlar	$U_T=\left[\frac{L_{si}}{k_{si}}+\frac{L_T}{k_T}\right]^{-1}$	(12)
Convection Factor	$h_{conv}=2.8+3V$	(13)
Radiation Factor	$h_{rad}=\varepsilon_g\sigma(T_{sky}+T_{cell})(T^2{}_{sky}+T^2{}_{cell})$	(14)
Sky Temperature	$T_{sky}=T_{amb}-6$	(15)
Collector Efficiency Factor	$F'=\frac{1}{1+\frac{U_{tT}w}{h_{f,T-a}(w-2t_d)+2k_{Al}mt_d\tanh(mL_c)}}$	(16)
Heat Removal Factor	$F_R=\frac{\dot{m}C_p}{U_{tT}bL}\left[1-exp\left(\frac{-bF'U_{tT}}{\dot{m}c_p}L\right)\right]$	(17)
Convection heat transfer coefficient	$h_{f,T-a}=\frac{Nu_D K}{D_e}$, $h_{f,Al-a}=h_{f,T-a}$	(18)
Nusselt number in constant temperature condition	$\begin{cases}Re_D\le 2100 & Nu_D=3.657\\ Re_D\ge 2100 & Nu_D=0.022Re^{0.8}Pr^{0.5}\end{cases}$	(19)

TABLE 4. Five Parameter Photovoltaic Model including constraint equations and the electrical efficiency [8, 11, 15]

Title	Equations	No.
Five Parameter Photovoltaic Model	$I=I_L-I_o\left[exp\left(\frac{V+IR_s}{a}\right)-1\right]-\frac{V+IR_s}{R_{sh}}$	(20)
@ short circuit current	$I=I_{sc,ref}, V=0$	(21)
@ open circuit voltage	$I=0, V=V_{oc,ref}$	(22)
@ maximum power point	$I=I_{mp,ref}, V=V_{mp,ref}$	(23)
@ maximum power point	$[d(IV)/dV]_{mp}=0$	(24)
@ short circuit current	$[dI/dV]_{sc}=-1/R_{sh,ref}$	(25)
Electrical Efficiency	$\eta_{el}=\frac{p_{mp}-P_{fan}}{A_{mod}\times G}\times 100$	(26)
Maximum Output Power	$p_{mp}=I_{mp}\times V_{mp}$	(27)

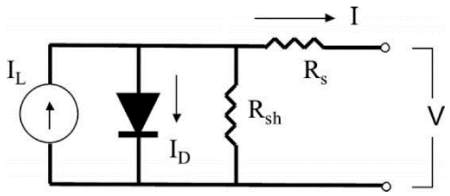

Figure 4. The equivalent electrical circuit of the solar cell [9]

3. 3. Exergy and Energy Analysis of MCPV/T Collector Exergy analysis is a technique that uses energy and mass conservation law and the second law of thermodynamics for the purposes of analyzing, designing and improving the energy of systems. Exergy is defined as the maximum amount of work that can be generated by a system or a flow of mass or energy that reaches the equilibrium state with the reference environment. According to the equations in Table 5, the general form of the equation of exergy equilibrium for a control volume in stable conditions is written as Equation (28) [19, 29]. The input and output exergy rates are given by the compressible fluid stream medium (here is the air) relative to the reference environment state by Equations (29) and (30) [19, 29]. The exergy rate of the heat transfer to the MCPV/T collector only includes the exergy rate of the solar radiation and, according to Petela theorem, is obtained from Equation (31) [19, 29]. In Equation (31), T_{sun} is the temperature of the sun in Kelvin and considered in the calculations 5774 °K [6]. The exergy rate of work consists related to the output electric power of the photovoltaic module reducing the consumed power of the fan(s) is calculated by the Equation (32) [16, 19, 30–32]. The exergy efficiency of the MCPV/T collector is defined as the net output exergy ratio to the desired input exergy of the control volume according to Equation (33) [19, 29]. By replacing Equations (29) and (32) within Equation (33), the exergy efficiency of the MCPV/T collector is obtained as Equation (34). In general, the complete reference for evaluating the performance of a PV/T collector is its overall efficiency [20]. To calculate the overall efficiency, the thermal efficiency equivalent to the electrical efficiency of the system is calculated in accordance with Equation (35) and summed up with the thermal efficiency of the system in accordance with Equation (36). To obtain overall efficiency, the electrical efficiency is divided by the thermal power efficiency of the region [20]. Considering the standard power plant thermal energy efficiency (C_f) value of about 0.36, the overall total PV/T efficiency can be calculated and measured in each experiment.

3. 4. Computational Simulation and Codes Developing Due to the dependence of the thermal analysis of the system on the electrical analysis, the simulations are carried out in the coupled thermal and electrical divisions. Thus, according to the algorithm used in Figure 5, the values of the parameters obtained from the experiment include ambient temperature, inlet fluid temperature, solar radiation, wind speed and flow rate of fluid, along with the geometric characteristics of the channel and the thermophysical properties of the various components of the system. These parameters are entered in the simulator code. Initially, the temperature of the solar cell and the electrical efficiency are assumed within nested loops of codes, then the cell temperature and electrical efficiency are finally accurately calculated.

In other words, during a repetitive process, the values obtained for solar cell temperature and electrical efficiency are compared with previous values.

TABLE 5. Efficiency equations including exergy, thermal and system overalls [6, 16, 19, 29–32]

Title	Equation	No.
Exergy balance equation in a steady-state condition	$\dot{E}x_Q - \dot{E}x_w + \dot{E}x_{in} - \dot{E}x_{out} - \dot{I}_{cv} = 0$	(28)
Exergy rate of Inlet mass	$\dot{E}x_{air,in} = \dot{m}C_p\left(T_{f,in} - T_{amb} - T_{amb}\,ln\left(\frac{T_{f,in}}{T_{amb}}\right)\right) + \dot{m}RT_{amb}\,ln\left(\frac{P_{f,in}}{P_{amb}}\right)$	(29)
Exergy rate of outlet mass	$\dot{E}x_{air,out} = \dot{m}C_p\left(T_{f,out} - T_{amb} - T_{amb}\,ln\left(\frac{T_{f,out}}{T_{amb}}\right)\right) + \dot{m}RT_{amb}\,ln\left(\frac{P_{f,out}}{P_{amb}}\right)$	(30)
Exergy rate of solar radiation intensity	$\dot{E}x_Q = \left[1 - \frac{4}{3}\left(\frac{T_{amb}}{T_{sun}}\right) + \frac{1}{3}\left(\frac{T_{amb}}{T_{sun}}\right)^4\right] \times (A_{mod} \times G)$	(31)
Network Exergy rate of outlet electrical power of PV	$\dot{E}x_W = V_{mp}I_{mp} - P_{fan}$	(32)
Exergy efficiency	$\eta_{ex} = \frac{Net\ Output\ Exergy}{Net\ Input\ Exergy} = \frac{\Delta\dot{E}x_a + \dot{E}x_w}{\dot{E}x_Q}$	(33)
Exergy efficiency	$\eta_{ex} = \frac{\dot{m}\left[C_p\left(T_{f,out} - T_{f,in} - T_{amb}\,ln\left(\frac{T_{out}}{T_{f,in}}\right)\right) - RT_{amb}\,ln\left(\frac{P_{f,out}}{P_{f,in}}\right)\right] + V_{mp}I_{mp} - P_{fan}}{(A_{mod} \times G)\left[1 - \frac{4}{3}\left(\frac{T_{amb}}{T_{sun}}\right) + \frac{1}{3}\left(\frac{T_{amb}}{T_{sun}}\right)^4\right]}$	(34)
Thermal efficiency equivalent of electrical efficiency	$\eta_{El-Th} = \frac{\eta_{el}}{C_f}$	(35)
Overall energy efficiency	$\eta_{ov} = \eta_{th} + \eta_{El-Th} = F_R\left[h_p(\alpha\tau)_{eff} - \frac{U_{tT}(T_{f,in} - T_{amb})}{G}\right] + \frac{V_{mp}I_{mp} - P_{fan}}{C_f(A_{mod} \times G)}$	(36)

Finally, after a few iterations, the final modified values are obtained. In the next step, considering the convergence of the concluded values, the simulated values of the fluid outlet temperature, the solar cell temperature, the current of the maximum electric power point, the maximum electric power point voltage, the electrical efficiency, the thermal efficiency, the overall efficiency and the exergy efficiency are accurately calculated. Of course, the values parameters of the laboratory data and those calculated from the simulation is calculated for simulator code of these parameters are also calculated against the results of experiments. Then, the RMS value of the computed validation using the MATLAB open-source-programming software. More specifically, in order to calculate the error of the values of simulation parameters relative to the laboratory values, the percentage of root mean square error (RMS) is calculated by Equation (37) [14]:

$$\mathrm{RMS} = \sqrt{\frac{\sum[100\times(X_{sim,i}-X_{exp,i})/X_{exp,i}]^2}{n}} \quad (37)$$

Table 6 contains the values of the required parameters to enter the simulator code. It should be noted that the values of the intensity of the solar irradiation, the ambient temperature, the temperature of the fluid inlet into the system, the flow rate of the fluid inlet and the velocity of the fluid in the channel from the experimental data were applied to the simulation code.

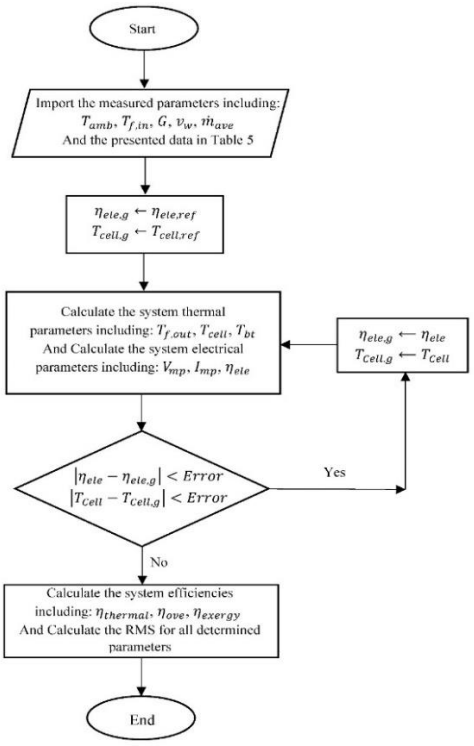

Figure 5. The calculation methodology for MCPV/T electrical and thermal parameters and exergy analysis

TABLE 6. MCPV/T system characteristics [11–14, 23, 24]

MCPVT Parameter	Value
PV module type	Polycrystalline Silicon-Glass to tedlar
L_1	$0.990\ m$
L_2	$0.680\ m$
$I_{sc,ref}$	$5.45\ A$
$V_{oc,ref}$	$21.60\ V$
$I_{mp,ref}$	$5.04\ A$
$V_{mp,ref}$	$17.86\ V$
$T_{cell,ref}$	$298.15\ K$
$\eta_{el,ref}$	0.1306
α	$0.0005\ A/°C$
β	$-0.0034\ V/°C$
G_{ref}	$1000\ \frac{W}{m^2}$
$T_{amb,ref}$	$298.15\ K$
L_g	$0.003\ m$
k_g	$1\ \frac{W}{mk}$
τ_g	0.95
ε_g	0.88
α_c	0.85
L_{si}	$300 \times 10^{-6} m$
K_{si}	$0.036\ \frac{W}{mk}$
α_T	0.5
L_T	$0.0005\ m$
K_T	$0.033\ \frac{W}{m.k}$
N_H	2
N_C	16
L	$0.486\ m$
W	$0.04\ m$
H	$0.02\ m$
t_d	$0.002\ m$
$K_{Al}(@\ 300K)$	$237\ \frac{W}{m.k}$
β_c	0.83
C_f	0.36

4. LABORATORY RESULTS AND VERIFICATION

The effect of a constant air flow rate of channels on the performance of the system was investigated. The system is located in coordinates (35° 44' 35" N, 50° 57' 25" E) to

the south and 35° from the horizon. The measurements were carried out in two different scenarios, differing in number of fans, ambient temperature, thermal, functional and electrical parameters were measured and recorded in a clear sunny atmosphere (blue sky) at time intervals of 30 minutes. Validation regarding the simulation is a need, which is done in MATLAB. For this purpose, a measurement plan is prepared to gather the relation variables data, which changed through the period of times. The results of the validation are shown in Figures 6, 7, 8 and 9.

Figure 6 shows the values of the measured parameters, including the intensity of the sun's radiation, wind speed and ambient temperature through with the test conditions for two modes of measuring one ON fan and three ON fans in the two consecutive days of October 2017.

Figure 7 shows the values of the measured and simulated parameters, including the temperature of the solar cell, the temperature of the back surface of Tedlar, and the fluid outlet temperature for the two states of one ON fan and three ON fans. In the test mode of one ON fan, the percentage of RMS for the solar cell temperature and the fluid outlet temperature were 6.02 and 2.90%, respectively. In the case of three ON fans test, the percentage of RMS for the solar cell temperature and the fluid outlet temperature were 8.53 and 3.13%, respectively, which indicates the appropriate consistency between the experimental and simulated values.

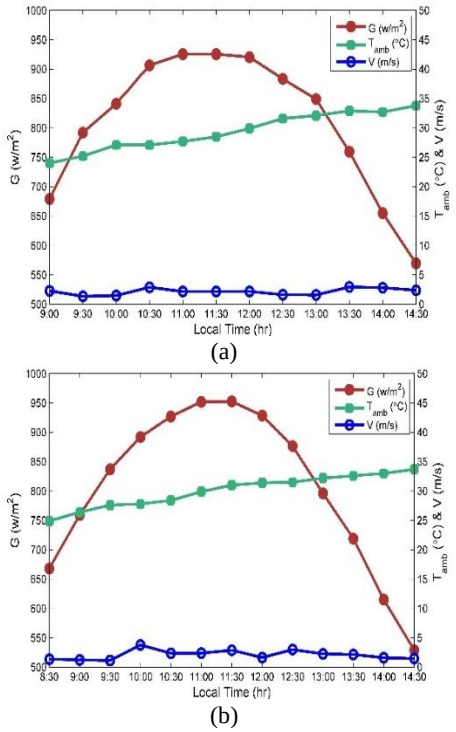

Figure 6. The irradiation, wind speed and ambient temperature per local time, (a): one ON fan and (b): three ON fans in the two consecutive days of October 2017

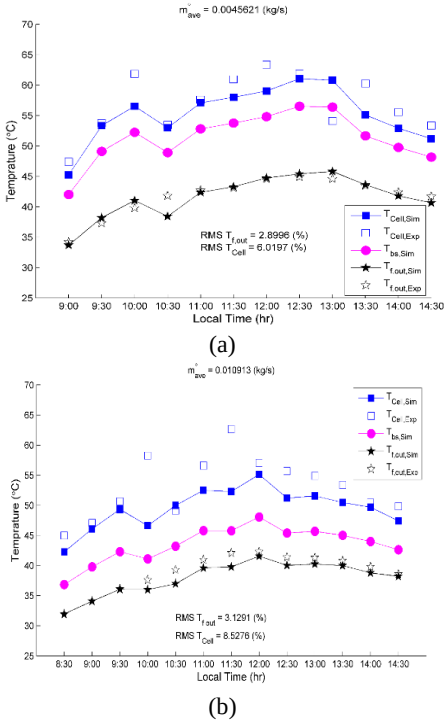

Figure 7. The measured and simulated temperatures of the solar cell, the back surface of Tedlar and outlet air medium at the two states of: (a) one ON fan and (b) three ON fans

Figure 8 shows the values of the current and voltage at the maximum point of the system output power for two modes of one ON fan and three ON fans. In the test mode of one ON fan, the percentage of RMS for the current at the maximum point of the system output power was 5.98% and for the voltage of the maximum power was 11.44%. In the case of three ON fans test, the percentage of RMS for the current at the maximum point of the system output power was 6.77% and for the voltage of the maximum power was 15.09%.

The values of overall energy, thermal, electrical and exergy efficiencies for two modes of one ON fan and three ON fans are demonstrated in Figure 9. In the test mode of one ON fan, the percentage of RMS for electrical efficiency, thermal efficiency, overall efficiency and exergy efficiency were 10.11, 9.90, 6.73, and 9.78%, respectively. In the test mode of three ON fans, the percentage of RMS for electrical efficiency, thermal efficiency, overall efficiency and exergy efficiency were 11.29, 12.72, 4.46 and 10.36% respectively. Also in this figure, as can be observed, the amount of thermal efficiency is much higher in terms of quantity than electrical efficiency. However, these two efficiencies are not homogeneous and according to Equation (35) in terms of the quality, the ratio of the thermal energy output ratio to the electrical energy output was 0.36. Based on this description and considering Equation (36), the effect of thermal energy efficiency on electric energy efficiency is higher.

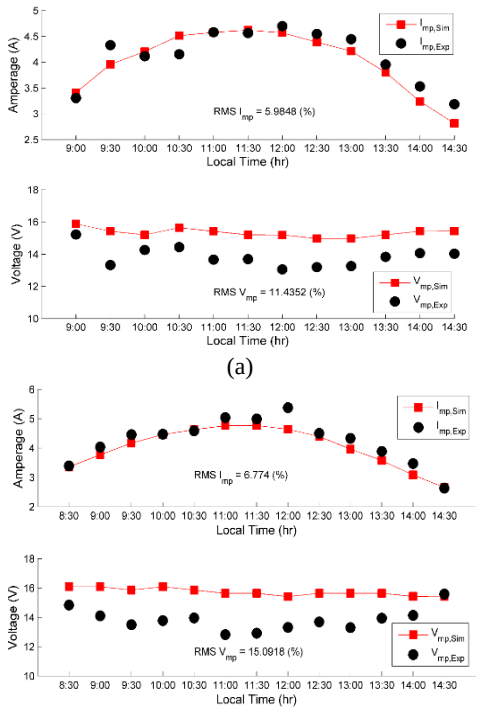

Figure 8. The measured and simulated values of current and voltage at the maximum power point of the system at the two states of: (a) one ON fan and (b): three ON fans

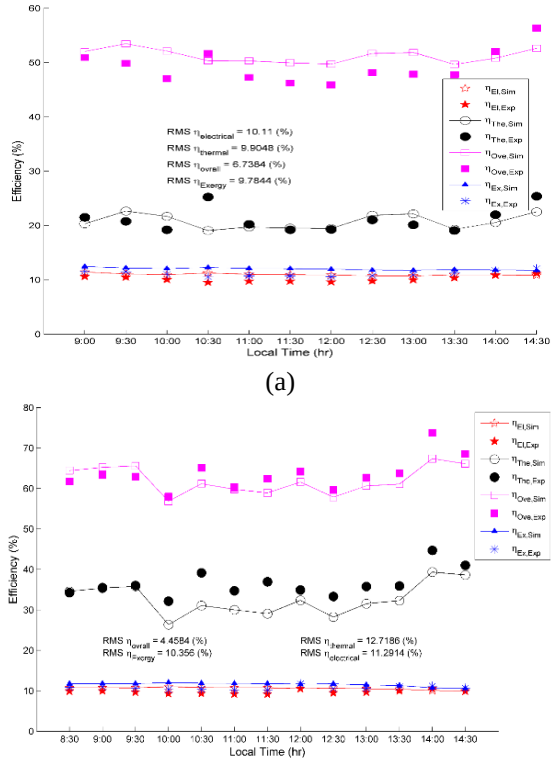

Figure 9. The measured and simulated values of overall energy, thermal, electrical and exergy efficiencies at the two states of: (a) one ON fan and (b): three ON fans

5. PARAMETRIC STUDY AND ANALYSIS TO ACHIEVE SYSTEM VARIATION BEHAVIOR

In this section, using the simulator program developed in the MATLAB programming software, the effect of different design, operational and environmental parameters on overall energy efficiency according to Equation (34) and exergy efficiency according to (36) of the MCPV/T collector, are studied. In order to study the effect of the change of each parameter on overall energy efficiency and exergy efficiency, other parameters such as intensity of solar irradiation, ambient temperature, the fluid inlet temperature of the system and constant wind speed are respectively equal to 800 W/m^2, 300 °K, 300 °K and 1 m/s.

5. 1. The Effect of Fan Location Two positions related to the fans are possible; the end and middle of air channels. The temperature of outlet air, overall efficiency and exergy efficiencies for both cases are shown in Figure 10-a to c.

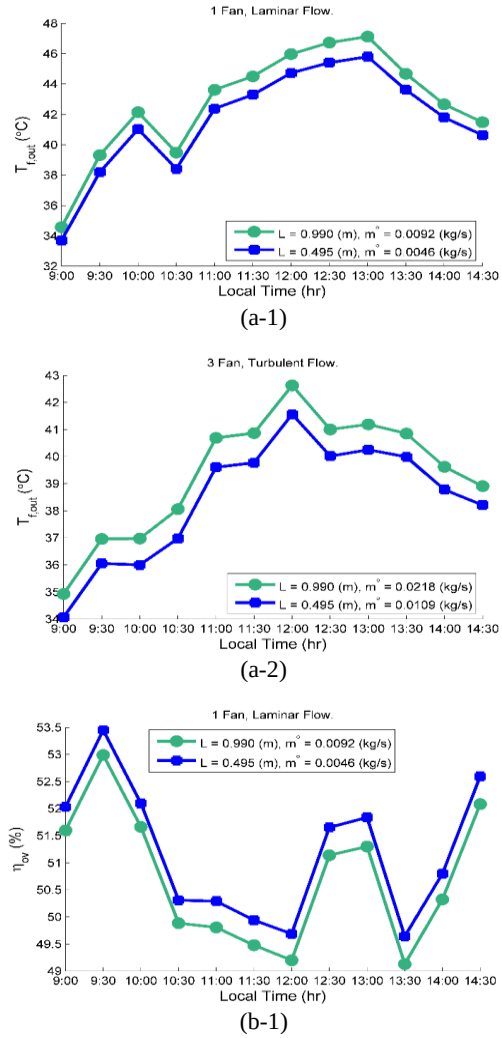

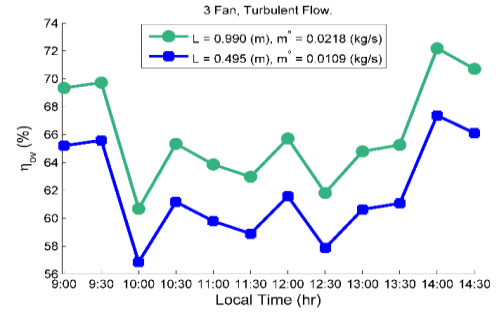

(b-2)

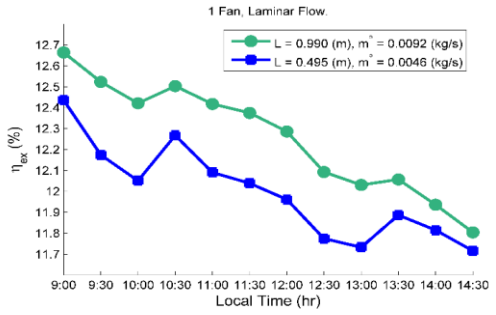

(c-1)

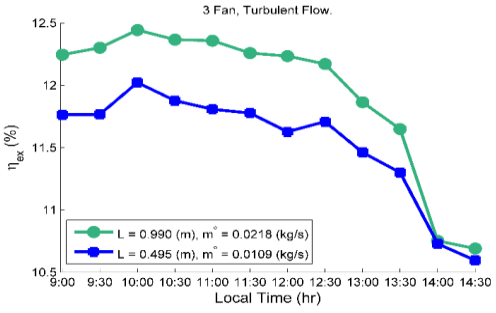

(c-2)

Figure 10. Comparison of simulated results based on fan localizing (a suction fan at the end or at the middle of the system), for two states of one ON fan and three ON fans. (a): Output air temperature profile, (b): Overall energy efficiency and (c): Exergy efficiency

Under the conditions of one ON fan, and where the suction fan is installed at the end of the system, the length of the flow channel increased from 0.495 m to 0.99 m and the average flow rate of the fluid increased from 0.0046 kg/s to 0.0092 kg/s. In both cases the flow regime is laminar. Under the conditions of the three ON fans and the the suction fan installed at the end of the system, the length of the flow channel increased from 0.495 m to 0.99 m; the average flow rate of the fluid increased from 0.0109 kg/s to 0.0218 kg/s, and the flow of fluid in both cases is turbulent.

As shown in Figure 10(a-1), in the case of one ON fan and using a suction fan at the end of the system relative to the middle of the system, due to the prolongation of the flow path, the fluid outlet temperature increased. In Figure 10(a-2), it is observed that in the case of three ON fans, when the suction fan is installed at the middle of the system, the temperature of the fluid outlet is increased compared to the middle of the system. First, this is due to the prolongation of the fluid path and secondly, increased flow rates in the turbulent flow regime. Here, the amount of heat transfer coefficient increases which will result in receiving more useful energy.

In general, Figure 10(a) shows that the average output fluid temperature is higher in the case of one ON fan (laminar flow regime) compared to three ON fans (turbulent flow regime). In other words, in the turbulent stream regime, due to the higher heat transfer coefficient, the fluid can receive more useful thermal energy from the photovoltaic module and will reduce the average working temperature of the system and achieving more in cooling target of the solar cell.

As shown in Figure 10(b-1), in the case of one ON fan and using a suction fan at the end of the system relative to the middle of the system, the overall system efficiency is reduced. This is due to the fact that the flow regime has not changed and is still laminar, which results in constant convection coefficient. Also, doubling the flow path of the fluid, and consequently increasing the area of the energy received from the sunlight, it has not been able to receive enough heat relative to the increase in the surface and the temperature of the solar cell is still high. In Figure 10(b-2), it is observed that in the three-fan mode, with the use of suction fan at the end of the system relative to the middle of the system, the overall efficiency of the system has increased. In fact, since the increase in the surface area of the energy received from the sunlight, it has been able to receive enough useful heat and causes more achieving in the cooling target of the solar cell.

In general, Figure 10(b) shows that, in the case of a three-fans state (turbulent stream regime), the overall system efficiency is higher. In fact, the heat carrier fluid has been able to obtain more heat energy from the photovoltaic module. Firstly, it will cool the photovoltaic module and increase electrical efficiency. Secondly, the thermal efficiency of the system is also increased due to the greater thermal energy absorbed by the system.

As shown in Figure 10(c-1), in the case of one ON fan and under conditions of use of the suction fan at the end of the system relative to the middle of the system, the exergy efficiency of the system has increased. In fact, due to the increase in the temperature of the output fluid, the mass flow could receive higher enthalpy and overall, the system can produce more useful work.

In Figure 10(c-2), similar to Figure 10(c-1), and in addition, generating more electrical power due to the cooling of solar cells, the system can produce higher useful work, and exergy efficiency of the system has increased. Figure 10(c) indicates that the average magnitude of the exergy efficiency is almost equal for two modes of one ON fan and three ON fans, but in general, the average exergy of ON fan is a bit higher. The

reason is that, firstly, the fluid outlet temperature in the case of one ON fan is higher, which due to the increase in the enthalpy of the heat carrier fluid, it will result in more useful work. Secondly, in the case of using three ON fans, the electric power consumption of the fans, which reduces 5.76 watts, is nearly three times more compared to the case of one ON fan which is equal to 1.92 watts. Increasing the electrical energy consumption will reduce the electrical efficiency of the photovoltaic module and, consequently, decrease the efficiency of the exergy.

5. 2. Effect of Mass Flow Rate, Flow Channel Height and Combined Simultaneously Effect of Two Parameters In Figure 11(a), it can be seen that with increasing input flow velocity, the overall energy efficiency increases. With a further increase in the fluid flow rate of 0.05 kg/s, the overall energy efficiency was almost constant and equal to 80%. Therefore, the effect of increasing the flow rate of the fluid is negligible. However, the exergy efficiency is initially increased by increasing this parameter, and decreases when it reaches a maximum at its optimal local point equal to 13.46% (fluid flow rate equal to 0.024 kg/s). This is due to the fact that increasing the speed of the inlet fluid increases the pressure drop in the flow path and the power consumption of the fans and reduces the exergy efficiency.

As shown in Figure 11(b), the overall energy efficiency decreases with increasing channel height and reaches a constant value of 70%. When the fluid flow height increases the fluid outlet temperature decreases; therefore, the thermal efficiency decreases; that is due to the lack of proper cooling of the photovoltaic module, the electrical efficiency decreases and the overall energy efficiency is reduced as a result of these two mentioned reasons. At the same time, with the increase in the height of the channel, the exergy efficiency is first increased and then it changed its behavior and decreased. This decrease is taking place just after achieving the maximum optimal value of 13.64% (regards to the height of the channel equal to 0.011 m). In the area before the optimal point, the amount of pressure drop is very high and results in loss of exergy efficiency. At the same time, in the region after the optimal point, decreased output fluid temperature will again decrease the exergy efficiency.

In Figures 11(c) and 11(d), the effects of simultaneous changes in the flow rate of the fluid (in the range of 0.001 to 0.045 kg/s) and the height of the channel (in the range of 0.005 to 0.05 m) with constant value of other system variables on the overall energy efficiency and exergy efficiency have been demonstrated. As shown in Figure 11(c), the maximum overall energy efficiency values will occur in low channel heights and high values of fluid flow rates and the function of the overall energy efficiency drawn have ascending behavior within the specific range.

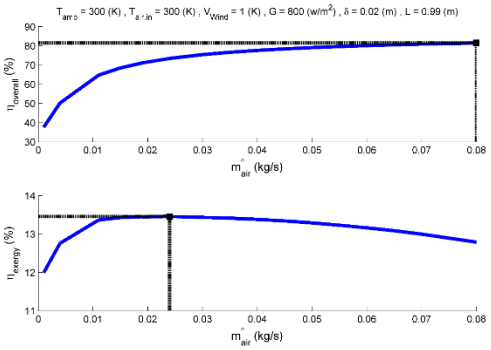

(a)

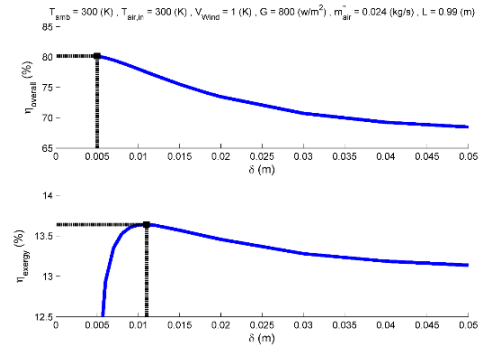

(b)

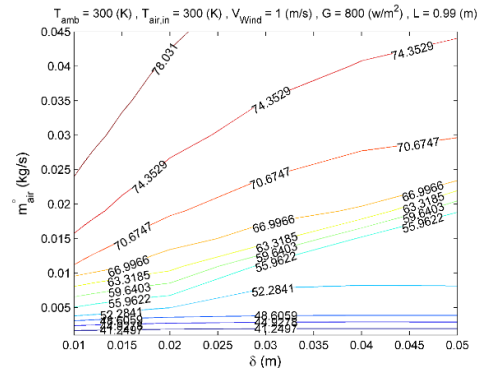

(c)

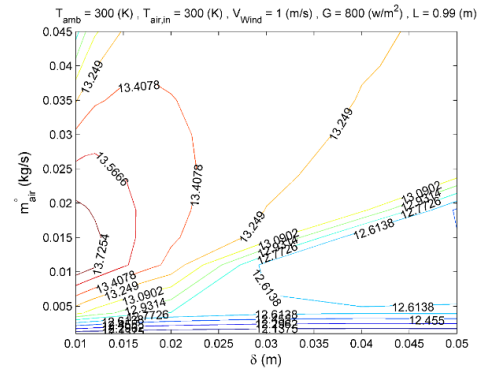

(d)

Figure 11. Changes of overall energy and exergy efficiencies versus: (a) Air flow rate, (b) Height of the channel; (c) Simultaneously effect of air flow rate and height of channels on overall efficiency and (d) Simultaneously effect of air flow rate and height of channels on exergy efficiency

This is while in Figure 11(d), according to the aligned lines, the amount of exergy efficiency in the regions with lower channel height is maximum and the exergy efficiency function has two local extremum regions, at the fluid flow rate equals to 0.011 kg/s, and a flow channel height of 0.006 m has its maximum value of 14.04%. Also, in these conditions, the amount of energy efficiency is calculated as 73.05%.

In Table 7, the results of thermal, electrical and overall efficiencies for a summary of references investigating air-cooled PV/T system and the present study are presented.

Indeed, Table 7 is a one-page comparison point of view and explains the achievement of this work in comparison with other similar researches that are investigated in the literature survey. The concept that separates finding of the present study is a consideration on laminar and turbulent heat transfer in different case of outcome variables such as irradiation and temperature.

TABLE 7. Comparison of the results of the present study with a previous works

Ref.	Year	Thermal efficiency (%)	Electrical efficiency (%)	Overall efficiency (%)	Exergy efficiency (%)	Description
Present study	-	20.21% (One fan) 39.14% (Three fans)	9.73% (One fan) 9.35% (Three fans)	47.24% (One fan) 65.10% (Three fans)	10.72% (One fan) 10.40% (Three fans)	Modelling and analysis of an innovative multi-channel photovoltaic/thermal (MCPV/T) system with experimental measurements including 16 open-air aluminum channels for air medium flow purposes on both one and three fan mode.
[11]	2006	-	-	16%	-	Performance investigation of the PV module integrated with air duct for the composite climate of India by using thermal model and laboratory testing.
[12]	2009	15.7-18.3% (Glass-to-glass) 13.4-16.5% (Glass-to-tedlar)	9.5-11%	43.4-47.4% (Glass-to-glass) 41.6-45.4% (Glass-to-Tedlar)	-	Analytical solution and laboratory testing for performance comparison of two types of photovoltaic (PV) module namely PV module with Glass-to-Tedlar and Glass-to-Glass.
[13]	2010	17.18%	10.01%	45%	10.75%	Analytical expression and experimental testing of single-channel PV/T system.
[25]	2013	18%	3.9%	28%	-	Double pass hybrid (PV/T) solar air heater with slats (DPHSAH)
[26]	2012	55%	8-14%	-	-	A parallel array of ducts with inlet/outlet manifold designed for uniform airflow distribution which attached to the back of the PV panel, with and without active cooling.
[33]	2016	50%	15%	-	12-41%	Experimental study of applying the PVT solar systems in Tunisian houses and buildings on both passive and active mode.
[34]	2016	56.19%	13.75%	-	-	The analytical expression derived from the energy balance equations for the system components and experimental testing of an air single pass collector which was reformed with a number of thin rectangular fins.
[35]	2017	19%	12.8%	13.4%	12-13.8%	A thermal model for semitransparent PVT with thermoelectric cooler (PVTTEC) collector derived from overall energy balance maintained by each component of the semitransparent.
[36]	2018	21.3-82.9%	9.87-11.34%	31.2–94.2%	11.72-13.06%	Evaluation of Steady-state on photovoltaic thermal (PVT) collector with ∇-groove by using the analytical and the matrix inversion methods with experimental studies.

6. CONCLUSION

An analytical expression at one-dimensional steady-state boundary conditions has been performed to investigate the solution of PV/T system thermal and electrical behaviors. A proper agreement is achieved between simulation and experimental results. Furthermore, with a complex of a parametric study the items namely, maximum outlet air temperature, overall energy and exergy efficiencies has been derived based on scenarios of laminar fluid flow, turbulent fluid flow and laminar fluid flow, respectively. Also, in turbulent fluid flow, when the position of fans are at the end of the channels, the values of outlet air temperature, overall energy and exergy efficiencies are more appropriate in compare with the other position of fans. However, opposed to laminar fluid flow, the fans' position in the middle, regards more appropriate results in overall energy efficiency. The effect of other parameters has been investigated on total energy efficiency and exergy efficiency when one parameter is variable and the others are constant. The values of pressure loss, as the fans power consumption and total energy efficiency increase based on the fluid flow rate increases. The mentioned value decreases to a constant value with the increase of channel depth. In the case of exergy efficiency, it is issued that the local optimum point is declared over the change of fluid flow rate and channel depth. In this research, a heat exchanger at the extending surface is developed with the concept of 72.19% overall energy efficiency and 12.66% exergy efficiency at experimental test condition.

In this research, the following results have been obtained:

(1) The thermal efficiency, electrical efficiency, overall energy efficiency and exergy efficiency of the MCPV/T system under ambient test conditions of one ON fan were 20.21, 9.73, 47.24 and 10.72%, respectively and under the conditions of three ON fans were 39.14, 9.35, 65.10, and 10.40%, respectively. The use of three fans will increase the flow rate of the fluid and turn the flow regime into turbulent which cools the system, and at the same time increases the thermal efficiency and overall energy efficiency. Due to the increased power of the fan in the three-fan mode, the average electrical efficiency is reduced by 0.74% compared to one fan mode, which reduces the exergy efficiency. To overcome this problem, a low-power fan can be used within a MCPV/T system in a higher surface area, the problem of high fan power consumption will be eliminated due to higher power output.

(2) The RMS values of overall energy and exergy efficiencies in the conditions of one ON fan are 6.73 and 9.78% respectively, and in the case of three ON fans, it is 4.46 and 10.36%, respectively, which is consistent with previous studies. Therefore, a parametric solution to predict the system response to overall energy and exergy efficiency has been used.

(3) In the state of one ON fan (laminar flow regime) in the system compared to three ON fans (turbulent flow regime), the average fluid temperature is higher and the total system energy efficiency is lower. The average magnitude of the exergy efficiency for the two states is almost equal, but the average of the exergy of the one ON fan mode is higher to a small extent.

(4) Under fan positioning conditions at the end of the system compared to the middle of the system and in the presence of one fan, the fluid outlet temperature and exergy efficiency increase and the overall energy efficiency decreases. Under the same conditions with three fans, the fluid outlet temperature, the exergy efficiency, and the overall energy efficiency of the system have increased.

(5) By increasing the flow rate, the overall energy efficiency increases to a constant value of 80% and the amount of exergy efficiency has a local maximum value of 13.46% at a fluid flow rate of 0.024 kg/s. With increasing channel height, the overall energy efficiency decreases and reaches a constant value of 70% and the exergy efficiency has a local maximum value of 13.64% at the channel height of 0.011 m.

7. ACKNOWLEDGMENT

The present study is supported by the Materials and Energy Research Center (MERC) through grant No. 571394054. Authors are acknowledged for the supports.

8. REFERENCES

1. Salih, S.M., Jabur, Y.K. and Kadhim, L. A., "Analysis of Temperature Effect on a Crystalline Silicon Photovoltaic Module Performance", ***International Journal of Engineering-Transactions B: Applications***, Vol. 29, No. 5, (2015), 722–727.
2. Kalogirou, S.A. and Tripanagnostopoulos, Y., "Hybrid PV/T solar systems for domestic hot water and electricity production", ***Energy Conversion and Management***, Vol. 47, No. 18–19, (2006), 3368–3382.
3. Reddy, S.R., Ebadian, M.A. and Lin, C. X., "A review of PV–T systems: Thermal management and efficiency with single phase cooling", ***International Journal of Heat and Mass Transfer***, Vol. 91, (2015), 861–871.
4. Kasaeian, A.B., Mobarakeh, M.D., Golzari, S. and Akhlaghi, M. M., "Energy and Exergy Analysis of Air PV/T Collector of Forced Convection with and without Glass Cover", ***International Journal of Engineering-Transactions B: Applications***, Vol. 26, No. 8, (2013), 913–926.
5. Kalogirou, S.A., Solar energy engineering: processes and systems, Academic Press, (2013).
6. Duffie, J.A. and Beckman, W.A., Solar engineering of thermal processes, John Wiley & Sons, (2013).
7. Kern, E.C. and Russell, M.C., Hybrid photovoltaic/thermal solar energy system, Report No. COO-4577-1, Lexington, USA, (1978).

8. Tripanagnostopoulos, Y., Photovoltaic/thermal solar collectors, Elsevier Ltd, (2012).
9. De Soto, W., Klein, S.A. and Beckman, W. A., "Improvement and validation of a model for photovoltaic array performance", ***Solar Energy***, Vol. 80, No. 1, (2006), 78–88.
10. Zondag, H.A., de Vries, D.D., Van Helden, W.G.J., van Zolingen, R.C. and Van Steenhoven, A. A., "The thermal and electrical yield of a PV-thermal collector", ***Solar Energy***, Vol. 72, No. 2, (2002), 113–128.
11. Tiwari, A., Sodha, M.S., Chandra, A. and Joshi, J. C., "Performance evaluation of photovoltaic thermal solar air collector for composite climate of India", ***Solar Energy Materials and Solar Cells***, Vol. 90, No. 2, (2006), 175–189.
12. Joshi, A.S., Tiwari, A., Tiwari, G.N., Dincer, I. and Reddy, B. V., "Performance evaluation of a hybrid photovoltaic thermal (PV/T)(glass-to-glass) system", ***International Journal of Thermal Sciences***, Vol. 48, No. 1, (2009), 154–164.
13. Sarhaddi, F., Farahat, S., Ajam, H., Behzadmehr, A.M.I.N. and Adeli, M. M., "An improved thermal and electrical model for a solar photovoltaic thermal (PV/T) air collector", ***Applied Energy***, Vol. 87, No. 7, (2010), 2328–2339.
14. Amori, K.E. and Al-Najjar, H. M. T., "Analysis of thermal and electrical performance of a hybrid (PV/T) air based solar collector for Iraq", ***Applied Energy***, Vol. 98, (2010), 384–395.
15. Tonui, J.K. and Tripanagnostopoulos, Y., "Improved PV/T solar collectors with heat extraction by forced or natural air circulation", ***Renewable Energy***, Vol. 32, No. 4, (2007), 623–637.
16. Petela, R., "Exergy of undiluted thermal radiation", ***Solar Energy***, Vol. 74, No. 6, (2003), 469–488.
17. Chow, T.T., Pei, G., Fong, K.F., Lin, Z., Chan, A.L.S. and Ji, J., "Energy and exergy analysis of photovoltaic–thermal collector with and without glass cover", ***Applied Energy***, Vol. 86, No. 3, (2009), 310–316.
18. Sarhaddi, F., Farahat, S., Ajam, H. and Behzadmehr, A., "Exergetic performance assessment of a solar photovoltaic thermal (PV/T) air collector", ***Energy and Buildings***, Vol. 42, No. 11, (2010), 2184–2199.
19. Sobhnamayan, F., Hamidi, A., Monavari, H.R., Sarhaddi, F., Farahat, S. and Alavi, M. A., "Performance evaluation of a solar photovoltaic thermal air collector using energy and exergy analysis", ***Journal of Renewable and Sustainable Energy***, Vol. 3, (2011), 043115(1–16).
20. Joshi, A.S. and Tiwari, A., "Energy and exergy efficiencies of a hybrid photovoltaic–thermal (PV/T) air collector", ***Renewable Energy***, Vol. 31, No. 13, (2007), 2223–2241.
21. Robles, A., Duong, V., Martin, A.J., Guadarrama, J.L. and Diaz, G., "Aluminum minichannel solar water heater performance under year-round weather conditions", ***Solar Energy***, Vol. 110, (2014), 356–364.
22. Jin, G.L., Ibrahim, A., Chean, Y.K., Daghigh, R., Ruslan, H., Mat, S., Othman, M.Y. and Sopian, K., "Evaluation of single-pass photovoltaic-thermal air collector with rectangle tunnel absorber", ***Recent Advances in Applied Mathematics***, Vol. 7, No. 2, (2010), 493–498.
23. Tabet, I., Touafek, K., Bellel, N. and Khelifa, A., "Thermal performances of vertical hybrid PV/T air collector", ***The European Physical Journal Plus***, Vol. 131, No. 410, (2016), 1–15.
24. Fan, W., Kokogiannakis, G., Ma, Z. and Cooper, P., "Development of a dynamic model for a hybrid photovoltaic thermal collector–Solar air heater with fins", ***Renewable Energy***, Vol. 101, (2017), 816–834.
25. Srinivas, M. and Jayaraj, S., "Performance study of a double pass, hybrid-type solar air heater with slats", ***International Journal of Energy Engineering***, Vol. 3, No. 4, (2013), 112–121.
26. Teo, H.G., Lee, P.S. and Hawlader, M. N. A., "An active cooling system for photovoltaic modules", ***Applied Energy***, Vol. 90, No. 1, (2012), 309–315.
27. Solanki, S.C., Dubey, S. and Tiwari, A., "Indoor simulation and testing of photovoltaic thermal (PV/T) air collectors", ***Applied Energy***, Vol. 86, No. 11, (2009), 2421–2428.
28. Dubey, S., Sandhu, G.S. and Tiwari, G. N., "Analytical expression for electrical efficiency of PV/T hybrid air collector", ***Applied Energy***, Vol. 86, No. 5, (2009), 697–705.
29. Bejan, A., Advanced engineering thermodynamics, John Wiley & Sons, (2016).
30. Sahin, A.D., Dincer, I. and Rosen, M. A., "Thermodynamic analysis of solar photovoltaic cell systems", ***Solar Energy Materials and Solar Cells***, Vol. 91, No. 2–3, (2007), 153–159.
31. Petela, R., "An approach to the exergy analysis of photosynthesis", ***Solar Energy***, Vol. 82, No. 4, (2008), 311–328.
32. Joshi, A.S., Dincer, I. and Reddy, B. V., "Thermodynamic assessment of photovoltaic systems", ***Solar Energy***, Vol. 83, No. 8, (2009), 1139–1149.
33. Hazami, M., Riahi, A., Mehdaoui, F., Nouicer, O. and Farhat, A., "Energetic and exergetic performances analysis of a PV/T (photovoltaic thermal) solar system tested and simulated under to Tunisian (North Africa) climatic conditions", ***Energy***, Vol. 107, (2016), 78–94.
34. Mojumder, J.C., Chong, W.T., Ong, H.C. and Leong, K. Y., "An experimental investigation on performance analysis of air type photovoltaic thermal collector system integrated with cooling fins design", ***Energy and Buildings***, Vol. 130, (2016), 272–285.
35. Dimri, N., Tiwari, A. and Tiwari, G. N., "Thermal modelling of semitransparent photovoltaic thermal (PVT) with thermoelectric cooler (TEC) collector", ***Energy Conversion and Management***, Vol. 146, (2017), 68–77.
36. Fudholi, A., Zohri, M., Jin, G.L., Ibrahim, A., Yen, C.H., Othman, M.Y., Ruslan, M.H. and Sopian, K., "Energy and exergy analyses of photovoltaic thermal collector with ∇-groove", ***Solar Energy***, Vol. 159, (2018), 742–750.

Energy and Exergy Evaluation of Multi-channel Photovoltaic/Thermal Hybrid System: Simulation and Experiment

A. Hosseini Rad[a], H. Ghadamian[a], H. R. Haghgou[a], F. Sarhaddi[b]

[a] *Department of Energy, Materials and Energy Research Center (MERC), Tehran, Iran*
[b] *Department of Mechanical Engineering, University of Sistan and Baluchestan, Zahedan, Iran*

P A P E R I N F O

Paper history:
Received 22 July 2019
Received in revised form 17 August 2019
Accepted 12 September 2019

Keywords:
Computational Modeling
Exergy and Energy Analysis
Multichannel System
Laminar and Turbulent Flows
Photovoltaic/ Thermal

چکیده

در این پژوهش به بررسی نمونه‌وار پایلوت و تحلیل یک سیستم فتوولتائیک حرارتی چند کاناله (MCPV/T) نوآورانه به همراه اندازه‌گیری محیطی در منطقه‌ی جغرافیایی با مختصات (35° 44' 35" N, 50° 57' 25" E) پرداخته شده است. این سیستم از یک‌پارچه‌سازی یک پنل فتوولتائیک و دو مبادله‌کن حرارتی چندکاناله تشکیل شده است. بازده‌های الکتریکی، اگزرژی و انرژی کلی سیستم در نرخ جریان سیال هوای ۰/۰۰۵ kg/s و شدت تابش ۹۲٦ W/m^2 به ترتیب ۹/۷۳٪، ۱۰/۷۲٪و ٤۷/۲٤٪ و در نرخ جریان سیال هوا ۰/۰۱۱ kg/s و شدت تابش ۹۲۷ w/m^2 به ترتیب ۹/۳۵٪، ۱۰/٤۰٪ و ۱۰/٦۵٪ به دست آمده است. بر اساس نتایج شبیه‌سازی که در تطابق مناسبی با نتایج حاصل از آزمون آزمایشگاهی می‌باشد، با افزایش نرخ جریان سیال هوا بازده انرژی کلی افزایش یافته و به یک مقدار حدی ۸۰٪ میل می‌کند، این در حالیست که مقدار بیشینه‌ی بازده اگزرژی دارای یک نقطه‌ی بهینه‌ی محلی ۱۳/٤٦٪ در نرخ جریان سیال ۰/۰۲٤ kg/s می‌باشد. به طور مشابه با افزایش ارتفاع مجرای جریان، بازده انرژی کلی کاهش یافته و به یک مقدار حدی ۷۰٪ میل می‌کند و بازده بیشینه‌ی اگزرژی دارای یک نقطه‌ی بهینه‌ی محلی ۱۳/٦٤٪ در ارتفاع مجرای جریان ۰/۰۱۱ m می‌باشد. به طور کلی می‌توان چنین گفت که سیستم در شرایط رژیم جریان آرام دارای کیفیت انرژی (راندمان اگزرژی) بالاتر و در شرایط رژیم جریان آشفته دارای کمیت انرژی (بازده انرژی) بالاتر است.

***doi**: 10.5829/ije.2019.32.11a.18*